

Research Article

# One-Dimensional Multi-Frequency Spectrometer

Christian Knopke<sup>a</sup> · Bradley W. Ficko<sup>a</sup> · Solomon G. Diamond<sup>a,b,\*</sup>

<sup>a</sup>Lodestone Biomedical LLC, Lebanon, New Hampshire, USA

<sup>b</sup>Thayer School of Engineering at Dartmouth, Hanover, New Hampshire, USA

\*Corresponding author, email: [Solomon.G.Diamond@Dartmouth.edu](mailto:Solomon.G.Diamond@Dartmouth.edu)

Received 17 March 2019; Accepted 09 July 2019; Published online 31 July 2019

© 2019 Knopke; licensee Infinite Science Publishing GmbH

This is an Open Access article distributed under the terms of the Creative Commons Attribution License (<http://creativecommons.org/licenses/by/4.0>), which permits unrestricted use, distribution, and reproduction in any medium, provided the original work is properly cited.

## Abstract

Magnetic Particle Spectroscopy (MPS) is an important measurement method to characterize the non-linear behavior of magnetic nanoparticles (MNPs). MPS systems provide valuable data for developing efficient magnetic particle imaging (MPI) methods and optimizing MNP contrast agents. We developed a multiple-excitation-coil spectrometer to recreate AC field patterns that are otherwise only found in 3D MPI systems. The presented Nanoparticle Characterization System (NCS) is capable of creating gradient fields and multi-frequency excitation fields as well as AC field-free-points. With its integrated sample mover, the NCS enables investigations into the effects of these field patterns on samples of  $> 0.1 \mu\text{g}$  iron mass in up to  $100 \mu\text{l}$  volume along one dimension.

## I. Introduction

### I.1. Spectrometer

In this paper we present a custom-built magnetic nanoparticle (MNP) spectrometer that is designed to accelerate the development of magnetic particle imaging (MPI) methods, contrast agents and biomarkers [1, 2]. It distinguishes itself from its commercially available counterparts through its measurement range and modes. At the core of the measurement system sits a recirculating liquid cooled five coil configuration (Figure 1). There are two independently-controlled excitation coils and three pick-up coils that can be read out individually with gradiometer compensation which is currently performed digitally in real-time processing. The signal generation and data readouts are achieved via high-end audio studio equipment and customized commercial digital audio workstation software.

Independent control of the two excitation coils enables the measurement system to generate a variety of AC

field conditions. By using a linear actuator that moves the sample along the central axis of gradiometer, the Nanoparticle Characterization System (NCS) can be used to study field conditions that are otherwise only found in 3D imaging systems. The system settings can be configured to generate a single or multi-frequency AC-signal. Currently, the main frequency can be set from 500 Hz to 1500 Hz at 20 mT. Higher frequencies up to 25000 Hz are feasible at a reduced field strength. Additional secondary frequencies can be added to the main frequency. The phase and gain of each frequency can be adjusted individually.

When the two excitation coils are set with opposing phase, an AC field-free-point (FFP) can be created at the center of the field of view. An AC FFP is a fixed location in space along the central axis of the spectrometer where the magnetic field strength is continuously zero due to destructive interference of the two AC fields of equal magnitude. Additionally, if the excitation coils are set to the same phase but different amplitudes then the AC FFP can be shifted outside of the field of view and an AC gradient

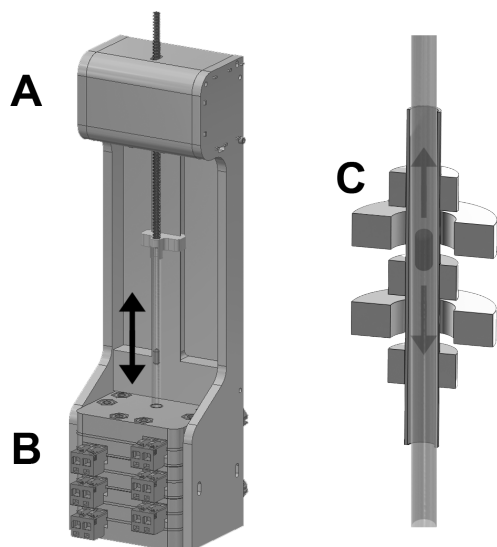


**Figure 1:** Illustration of one dimensional sample mover (A) with encased spectrometer (B). (C) Cross-section of the five coil configuration with sample-straw (diameter = 5.7 mm) in center.

field can be created. Furthermore, if the coils are set to arbitrary phases then irregular spatiotemporal patterns of AC gradients can be generated.

## I.II. Frequency Sweep and Linear Positioning

The NCS can support different measurement modes for a variety of applications. In this paper we present several measurement examples to illustrate the frequency sweep and linear positioning system of the spectrometer. The examples include two series of different concentrated MNP as well as an investigation of the particle binding state. Additionally, the option to generate an AC field free point is demonstrated.

## II. Materials

### II.I. Spectrometer Setup

The excitation and pickup coils were purchased from Jantzen Audio (Praestoe, Denmark). The temperature of the gradiometer is held constant with a P310 rack-mounted chiller from ThermoTek AG (Baden Baden, Germany). The AC signal generation and real-time processing is carried out with the REAPER digital audio workstation software and amplified with a Benchmark Media Systems AHB2 power amplifier (Syracuse, USA). The system's digital-to-analog converter and an analog-to-digital converter are also from Benchmark Media Systems (DAC3 DX; ADC16). The sample movement is performed with a non-captive NEMA 11 stepper motor from

Koco Motion US LLC (Morgan Hill, USA) that is controlled by a FP-Sigma programmable logic controller from Panasonic. The motor movement control was integrated into the REAPER audio software using a MIDI to CV converter (Pro SOLO MkII, KENTON). Analogously, the motor positioning feedback was integrated with a Pro CV to MIDI converter from KENTON (London, United Kingdom). The sample mover has a minimum step size of 0.05 mm and a stroke length of 50 mm.

### II.II. Nanoparticles and Beads

We obtained streptavidin-coated iron oxide MNP from Ocean Nanotech (San Diego, USA): SV0101. A sample of the Resovist precursor Ferucarbotran was obtained from Meito Sangyo (Tokyo, Japan). Note that alterations of the original magnetic signal of the Ferucarbotran are possible due to the age of the sample (Lot: DDM128N/S1-006, obtained October 2015).

Biotin coated polystyrene beads (PP-50-10) were obtained from Spherotech, Inc. (Lake Forest, USA). All samples were measured in 0.1 ml polypropylene PCR tubes (designed for Qiagen/Corbett Rotor-Gene) obtained from 4titude Limited (Wotton, United Kingdom).

## III. Results and Discussion

### III.I. Positioning sweep

The correct position of a sample within the central pickup coil is crucial to performing repeatable measurements. Even slight alterations in the sample position might change the signal readout.

To compensate for the influence of the sample position we implemented an automated positioning sweep that consists of the following steps: After the sample straw is placed into the holder a background measurement is carried out with the sample still outside of the measurement bore. The sample then traverses through the coil configuration while a measurement is performed every 2 mm over a total length of 44 mm. Each measurement takes 1 s. Based on this first sweep the position of the signal maximum is determined. In a second sweep the sample moved through the center of the signal maximum, this time over a distance of 9 mm with a measurement interval of 1 mm and a measurement time of 4 s per step. The total measurement time for this procedure is 112 s per sample.

In this experiment a series of Ferucarbotran samples with different iron concentrations from 5.9  $\mu\text{g}/\mu\text{l}$  (Figure 2: 1:10 dilution) down to 6 ng/ $\mu\text{l}$  (Figure 2: 1:10000 dilution) was measured. Each sample had a total volume of 20  $\mu\text{l}$ . The detected relative signal strength directly correlates to the amount of MNP per sample.

The lowest detectable amount of MNP was a 1:10000 dilution of the original Ferucarbotran, which contained

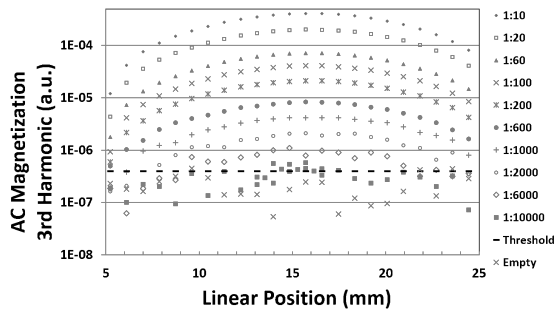


**Figure 2:** Magnetic signal of a Ferucarbotran concentration series during a linear sweep (1000 Hz, 20 mT). The detection threshold of the system is indicated at 4E-7.

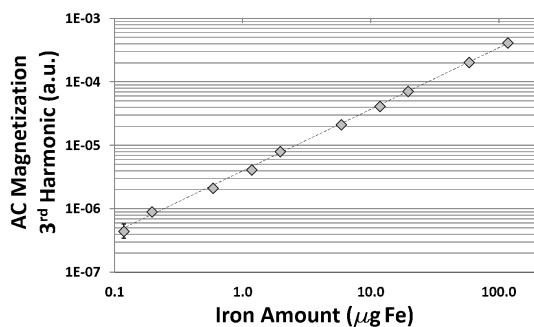


**Figure 3:** The total amount of nanoparticle iron per sample is displayed against the magnitude of the 3rd harmonic on a double logarithmic scale (1000 Hz, 20 mT).

120 ng of nanoparticle iron in the sample. The signal-to-noise ratio (SNR) for the NCS was calculated as the measured amplitude of the empty chamber pass through signal, which was calibrated to a mean of unity, relative to the standard deviation of the instrument noise. The resulting SNR values ranged from 138 dB to 148 dB depending on the harmonic channel. The contrast-to-noise ratio (CNR) for the 20  $\mu\text{l}$  sample of 1:10 diluted Ferucarbotran, computed from the highest measured signal for that sample to its detection limit was 68 dB. The SNR for the NCS is a measure of the system noise and stability whereas the CNR is sample-type dependent. In Figure 3 the correlation of the magnitude of the 3rd harmonic and the nanoparticle iron content is displayed. Because of this linear relationship MPS systems have been used to quantify MNP in different media [3] or in *in vitro* samples [4].

### III.II. Influence of Sample Volume on Magnetic Signal

Another application of the positioning sweep is to analyze the influence of the sample geometry. In an exemplary experiment we investigated the influence of the sample volume on the magnetic signal. Here, a series of

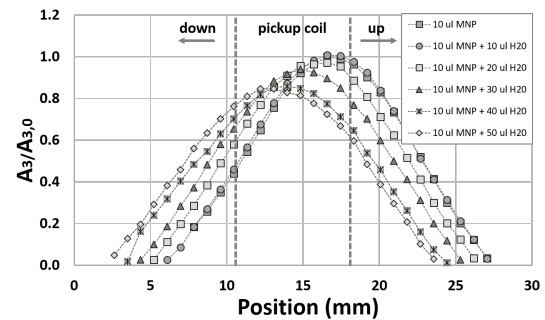


**Figure 4:** A series of six samples with different volumes, but same total iron content was measured (1000 Hz, 20 mT). Each sample contained 10  $\mu\text{l}$  of Ferucarbotran ( $m_{Fe} = 4 \mu\text{g}$ ) and only differed in the amount of water added. The size and position of the central pickup coil has been marked in the graphic. The magnetic signal of the third harmonic ( $A_3$ ) of each sample has been divided by the peak signal of the original sample ( $A_{3,0} = 10 \mu\text{l MNP}$ ).

six samples was measured using the linear sweep function. All samples contained the same amount of MNP (4  $\mu\text{g}$  of Ferucarbotran) and only varied in their total sample volume.

The linear sweep displayed in Figure 4 shows the signal change due to variations in total sample volume. Two effects become apparent with increasing sample volume: A noticeable decrease in signal intensity of the 3rd harmonic as well as a shift in peak position. The most diluted sample (10  $\mu\text{l MNP} + 50 \mu\text{l H}_2\text{O}$ ) exhibits a relative signal of only 85 % compared to the sample with the highest particle concentration (10  $\mu\text{l MNP}$ ). At the same time the peak signal position shifted from 16.5 mm to 13.1 mm.

Both effects can be attributed to the spatial distribution of the MNP in the sample. During the measurement the signal is generated when the sample is traversing between the upper and lower pickup coil with the highest signal generated when the sample passes the central pickup coil. Due to the shape of the sample tube a volume of 60  $\mu\text{l}$  takes up the space of a cylinder which is 11 mm high, but only 2.6 mm in diameter. The central pickup coil is only 8 mm in height and can therefore not fully cover the whole sample volume. Hence, a part of the signal reduction can be attributed to the filling factor of the sample in the pickup coil.

The change of the peak position can be explained by an elevation of the center of the magnetic moment due to filling the cylinder to higher levels.

### III.III. Frequency Sweep

A typical application of MPS systems is the analysis of the particle binding state. The particle's ability to follow an external magnetic field can be described by a superposition model [5] of Néel [6] and Brownian [7] relaxation. Immobilizing MNP through binding their ligands to sur-

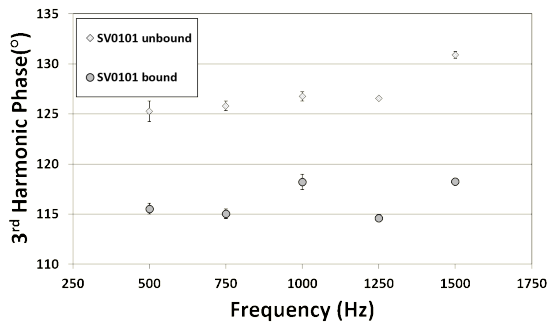


**Figure 5:** Phase of 3rd harmonic in bound and unbound state at 500 Hz, 750 Hz, 1000 Hz and 1500 Hz.

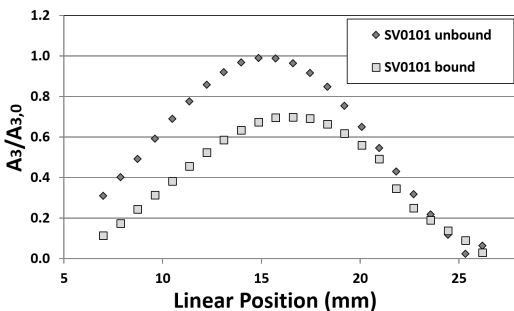


**Figure 6:** Linear sweep of SV0101 particles in bound and unbound state at 1500 Hz displayed as relative signal change of the 3rd Harmonic. The shift in the signal peak position can be attributed to sedimentation in bound state.

faces or cells inhibits the Brownian rotation and changes the effective relaxation time which in turn may affect the harmonic signal as shown in Figure 6.

The effective relaxation time can be measured with DC [8] and AC [9] methods and is dependent on the characteristics of the particles magnetic core, the binding state of the particle and the viscosity of the medium. To demonstrate the signal change between bound and unbound particles we immobilized a set of MNPs (100 nm in diameter) by adding 10  $\mu$ l of biotin coated polystyrene beads (5  $\mu$ m in diameter) and mixed them on a shaker for 1 h. In the subsequent measurement we analyzed the magnetic signal of the bound and unbound particles at 500 Hz to 1500 Hz in steps of 250 Hz. A frequency dependent signal change was found in the magnitude and phase of the 3rd harmonic. The phase is calculated relative to a digital generated reference tone and can be used as an indicator for nanoparticle binding events as it is generally independent of the MNP concentration (except high concentrations of specific MNP [10]).

Figure 5 shows the change in the phase of the 3rd harmonic for bound and unbound SV0101 particles. While the difference between the two states is approximately 10 degrees at 500 Hz, it increases to 12 degrees at 1500 Hz.

Even though the signal drop in the magnitude of the

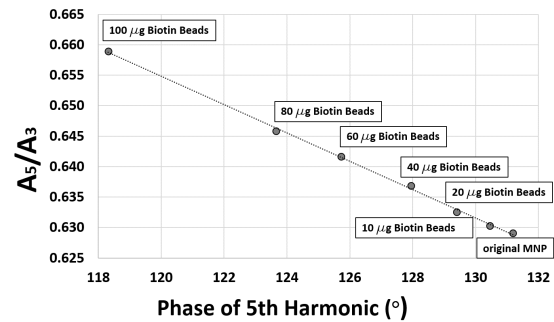


**Figure 7:** Series of streptavidin coated MNP (SV0101) with increasing amounts of biotin coated polystyrene beads (PP-50-10) measured at 1500 Hz. The increasing immobilization alters the phase of the 5th harmonic and the  $A_5/A_3$  ratio in a similar way. A trend line is added to show the linear dependency of the two parameters.

3rd harmonic is more pronounced than the phase change (Figure 6) it is an unfavorable indicator for particle binding. This is because the magnitude of the 3rd harmonic is also dependent on the total iron amount in the sample which might change in an *in vivo* setting. An alternative parameter that is independent of the total nanoparticle amount is the ratio of the 5th harmonic to the 3rd harmonic ( $A_5/A_3$ ). Like the phase the  $A_5/A_3$  ratio can be an indicator for changes in the relaxation time of the MNP [3, 9].

To demonstrate the sensitivity of phase as indicator of the MNP binding state we measured a series of streptavidin coated MNP (SV0101). Each sample contained 10  $\mu$ l of the undiluted nanoparticle solution as well as 10  $\mu$ l of biotinylated polystyrene beads (PP-50-10) containing various amounts of beads from 10  $\mu$ g to 100  $\mu$ g. In Figure 7 the alterations of the phase of the 5th harmonic and the  $A_5/A_3$  ratio due to changes in the binding state are displayed.

The phase of the 5th harmonic changes from 131 degrees for unbound particles to 118 degrees for bound particles. For the same samples, the  $A_5/A_3$  ratio changes by 3%. Similar changes were observed in the phases of the 3rd and 7th harmonic. The phase of the 5th harmonic stood out for its high contrast to noise ratio. The linear trend line indicates that the  $A_5/A_3$  ratio and the phase of the 5th harmonic are equally sensitive to the binding state of the particles.

### III.IV. Linear Positioning in Gradient Field

In this experiment we demonstrate the effects of an AC gradient field along one dimension with the help of the linear sample mover. In order to generate a gradient along the linear axis of the coil setup, the phase of the lower excitation coil was shifted by 180 degrees. The

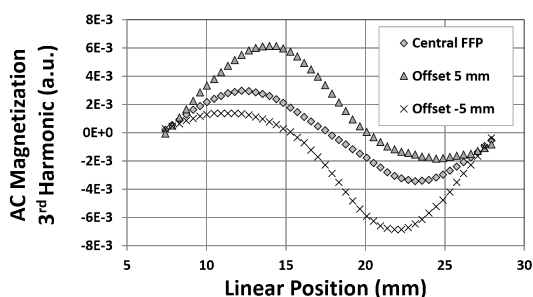


**Figure 8:** Magnetic Signal (3rd Harmonic) of 10  $\mu\text{l}$  liquid Ferucarbotran sample at 63 positions in an AC gradient field.

now opposing magnetic signals cancel each other out at the central pickup coil and create an AC field free point (FFP). This field pattern can be visualized with the help of an MNP sample (10  $\mu\text{l}$  Ferucarbotran) that traverses along the axis (Figure 8, Central FFP). The gradient at the central FFP is 1.6 mT/mm.

Alternative field patterns can be created through adjustments of the upper and lower excitation coils' field strength. Setting the one excitation coil to 15 mT and the opposing excitation coil to 25 mT shifts the position of the FFP approximately 5 mm in either direction.

Through the positioning sweep, the MNP responses in simple magnetic field patterns such as in AC field gradients can be studied in one dimension. The sample mover can also be used to study and improve the characteristics of the spectrometer. In the present results, the positioning sweep revealed that the magnetic AC signal of the two excitation coils is not perfectly symmetric due to slight variations in the coil placement.

## IV. Conclusions

The presented NCS coil arrangement demonstrated sensitivity to MNP mass in the 120 ng range. Through the individually controlled excitation coils, simple field patterns could be created and investigated along one dimension.

The frequency sweep option provides flexibility for studying the potential of MNP contrast agents in low-frequency imaging modalities. The frequency sweep can also be used to study the binding state of functionalized MNP. A system expansion to higher and lower frequencies would provide additional functionality. The fully integrated sample mover is a helpful addition for performing automated sample sweeps and to map MNP responses in simple magnetic field patterns. Through the positioning sweep the influence of the sample vol-

ume on the signal response could be visualized. These differences can now be addressed and taken into account when comparing different MNP samples.

## V. Outlook

The here applied digital gradiometer compensation removes electromagnetic interference that is common across the pickup coils. While the dynamic range of the ADCs was adequate for our initial applications, an analog compensation would increase the dynamic range of the system. We are currently developing an analog gradiometer setup with signal amplification which will be implemented in future systems.

## References

- [1] S. Biederer, T. Knopp, T. F. Sattel, K. Lüdtke-Buzug, B. Gleich, J. Weizenecker, J. Borgert, T. M. Buzug, and K. Lüdtke-Buzug. Magnetization response spectroscopy of superparamagnetic nanoparticles for magnetic particle imaging. *Journal of Physics D: Applied Physics*, 42(20):205007, 2009, doi:[10.1088/0022-3727/42/20/205007](https://doi.org/10.1088/0022-3727/42/20/205007).
- [2] D. Schmidt, M. Graeser, A. von Gladiss, T. M. Buzug, and U. Steinhoff. Imaging Characterization of MPI Tracers Employing Offset Measurements in a two Dimensional Magnetic Particle Spectrometer. *International Journal on Magnetic Particle Imaging*, 1(2), 2016, doi:[10.18416/IJMPI.2016.1604002](https://doi.org/10.18416/IJMPI.2016.1604002).
- [3] N. Löwa, M. Seidel, P. Radon, and F. Wiekhorst. Magnetic nanoparticles in different biological environments analyzed by magnetic particle spectroscopy. *Journal of Magnetism and Magnetic Materials*, 427:133–138, 2017, doi:[10.1016/j.jmmm.2016.10.096](https://doi.org/10.1016/j.jmmm.2016.10.096).
- [4] C. Gräfe, I. Slabu, F. Wiekhorst, C. Bergemann, F. von Eggeling, A. Hochhaus, L. Trahms, and J. H. Clement. Magnetic particle spectroscopy allows precise quantification of nanoparticles after passage through human brain microvascular endothelial cells. *Physics in Medicine and Biology*, 61(11):3986–4000, 2016, doi:[10.1088/0031-9155/61/11/3986](https://doi.org/10.1088/0031-9155/61/11/3986).
- [5] M. Shliomis. Effective viscosity of magnetic suspensions. *Zhurnal Eksperimentalnoi i Teoreticheskoi Fiziki*, 61:2411–2418, 1972.
- [6] Néel. Théorie du traînage magnétique des ferromagnétiques en grains fins avec application aux terres cuites. *Annales de Géophysique*, 5:99–136, 1949.
- [7] W. F. Brown. Thermal Fluctuations of a Single-Domain Particle. *Physical Review*, 130(5):1677–1686, 1963, doi:[10.1103/PhysRev.130.1677](https://doi.org/10.1103/PhysRev.130.1677).
- [8] D. Eberbeck, C. Bergemann, F. Wiekhorst, U. Steinhoff, and L. Trahms. Quantification of specific bindings of biomolecules by magnetorelaxometry. *Journal of Nanobiotechnology*, 6(1):4, 2008, doi:[10.1186/1477-3155-6-4](https://doi.org/10.1186/1477-3155-6-4).
- [9] A. M. Rauwerdink and J. B. Weaver. Concurrent quantification of multiple nanoparticle bound states. *Medical Physics*, 38(3):1136–1140, 2011, doi:[10.1118/1.3549762](https://doi.org/10.1118/1.3549762).
- [10] N. Löwa, P. Radon, O. Kosch, and F. Wiekhorst. Concentration Dependent MPI Tracer Performance. *International Journal on Magnetic Particle Imaging*, 2(1), 2016, doi:[10.18416/IJMPI.2016.1601001](https://doi.org/10.18416/IJMPI.2016.1601001).